Global Biogeochemical Cycles

RESEARCH ARTICLE
10.1029/2020GB006581

Arctic Continental Margin Sediments as Possible Fe and Mn Sources to Seawater as Sea Ice Retreats: Insights From the Eurasian Margin

Allyson Tessin[1,2], Christian März[2], Marie-Amélie Blais[3], Hans-Juergen Brumsack[4], Jens Matthiessen[5], Matt O'Regan[6], and Bernhard Schnetger[4]

[1]Department of Geology, Kent State University, Kent, OH, USA, [2]School of Earth and Environment, University of Leeds, Leeds, UK, [3]Department of Biology, Université Laval, Quebec City, Quebec, Canada, [4]Institute for Chemistry and Biology of the Marine Environment, University of Oldenburg, Oldenburg, Germany, [5]Alfred Wegener Institute, Bremerhaven, Germany, [6]Department of Geological Sciences, Stockholm University, Stockholm, Sweden

Abstract Continental margins are hot spots for iron (Fe) and manganese (Mn) cycling. In the Arctic Ocean, these depositional systems are experiencing rapid changes that could significantly impact biogeochemical cycling. In this study, we investigate whether continental margin sediments north of Svalbard represent a source or sink of Fe and Mn to the water column and how climate change might alter these biogeochemical cycles. Our results highlight that sediments on the Yermak Plateau and Sofia Basin exhibit accumulations of Fe and Mn phases compared to average shale. Conversely, sediments from the Barents Sea slope exhibit lower enrichments of Fe and Mn compared to average shale, with the exception of enriched, near-surface sediment layers. Pore waters from these slope sites provide evidence for Fe and Mn reduction and diffusion of Fe and Mn into near surface sediments, which are susceptible to physical or biogeochemical remobilization. These regional patterns are best explained by the spatial distribution of sea ice coverage and labile organic carbon fluxes to the seafloor. As sea ice continues to retreat and the Yermak Plateau becomes seasonally ice-free, productivity is expected to increase, which would increase the flux of carbon to the sediments, thereby increasing oxidant demand, and the reduction of Fe and Mn mineral phases. Our results suggest that as sea ice continues to retreat, the Yermak Plateau and other Arctic continental margins could become sources of Fe and Mn to Arctic bottom waters.

Key Points:
- Reactive iron and manganese are accumulated at Yermak Plateau sites but recycled at Barents Sea slope sites regardless of water depth
- Sea ice extent and export of surface carbon likely create different benthic oxidant demands, which drives differences in metal accumulation
- As sea ice extent and ocean currents change, the Yermak Plateau and other Arctic margins may become sources of metals to the water column

Supporting Information:
- Supporting Information S1

Correspondence to:
A. Tessin,
atessin@kent.edu

Citation:
Tessin, A., März, C., Blais, M.-A., Brumsack, H.-J., Matthiessen, J., O'Regan, M., & Schnetger, B. (2020). Arctic continental margin sediments as possible Fe and Mn sources to seawater as sea ice retreats: Insights from the Eurasian margin. *Global Biogeochemical Cycles*, *34*, e2020GB006581. https://doi.org/10.1029/2020GB006581

Received 17 FEB 2020
Accepted 22 JUN 2020
Accepted article online 20 JUL 2020

1. Introduction

Despite representing only 10% of the ocean's surface area and 0.5% of the ocean's volume, continental margins, which include the continental shelves, slopes, and rise, are global hot spots of biogeochemical carbon, nutrient, and metal cycling. As much as 90% of all of the marine organic carbon burial occurs within continental margin sediments (Liu et al., 2010). Continental margin sediments also act as a significant source of metals to the water column, such as Mn (Aller, 1994; Johnson et al., 1996; McManus et al., 2012) and Fe (Elrod et al., 2004; Johnson et al., 1999; Lam et al., 2006).

The cycling and transport of Fe and Mn are important for numerous marine biogeochemical processes. Both metals are micronutrients for phytoplankton. The importance of low Fe concentrations limiting primary productivity has been observed in many parts of the oceans (e.g., Moore et al., 2013; Tagliabue et al., 2017), including high-nutrient low-chlorophyll regions (e.g., Coale et al., 1998; Cullen, 1991; Johnson et al., 1997; Kuma et al., 1996; Martin & Fitzwater, 1988). Recently, Fe has been suggested to limit productivity in the Eurasian Arctic Ocean (Rijkenberg et al., 2018). Iron and, especially, Mn (oxyhydr)oxides are also efficient at scavenging (adsorbing) trace metals from seawater, meaning that the cycling of these minerals in near-surface sedimentary environments can exert a control on the cycling and transport of trace metals (Finney et al., 1984; Goldberg, 1954; Tessier et al., 1985). Iron (oxyhydr)oxides are also highly efficient sorbents of phosphate in the oceans and at the seafloor (Berner, 1973; Froelich et al., 1977; Slomp et al., 1996). Finally, Fe and Mn mineral phases likely play an important, yet poorly understood, role in the sedimentary preservation of organic matter (Barber et al., 2017; Estes et al., 2017; Johnson et al., 2015; Kaiser & Guggenberger, 2000; LaLonde et al., 2012).

The release of Mn and Fe from margin sediments to bottom waters from the seafloor is correlated to the amount of organic carbon oxidation within the sediments, with more Fe and Mn being remobilized when there is more oxidation of organic matter (Elrod et al., 2004; McManus et al., 2012). This creates an important link between the export of organic matter from the photic zone and the release of these metals from the seafloor. Generally, under oxic conditions, Fe and, particularly, Mn are sequestered as (oxyhydr)oxide phases (e.g., Johnson et al., 1996; Nameroff et al., 2002; Taylor & Macquaker, 2011). However, when sediments receive a sufficient amount of labile organic carbon, oxygen will be consumed within the surface sediments, and microbial Fe and Mn reduction become favorable metabolic pathways (Froelich et al., 1979). Following the dissolution of Fe and Mn (oxyhydr)oxides in oxygen-depleted sediment layers, dissolved Fe and Mn are released to the adjacent pore waters, where they can diffuse into oxygenated sediment layers and reprecipitate (e.g., Aller, 1990; Calvert & Pedersen, 1993; Emerson & Hedges, 2003). For Mn, this produces a near-ubiquitous surface enrichment in continental margin sediments and, in extreme cases, precipitation of Mn nodules (Calvert & Price, 1977).

Margin and shelf processes are especially important within the Arctic Ocean. Over half of the Arctic Ocean seafloor consists of continental shelves and margins (Jakobsson et al., 2003), and about 15% of global continental shelves are located within the Arctic (Menard & Smith, 1966). Arctic shelf and margin regions are characterized by more variable sea ice cover, higher biological productivity, stronger sediment resuspension, and more intense deposition/regeneration of organic matter than the deep basins of the central Arctic Ocean (Stein & Macdonald, 2004). Biogeochemical processes on shelves and margins dominate the Arctic carbon cycle (Liu et al., 2000; Macdonald et al., 2010) and, likely, the cycles of other elements as well. In these regions, the shuttling of Mn from shallow margin settings (<1,000 m) to deep basins (>1,000 m) is well documented (Macdonald & Gobeil, 2012). Many Arctic shelf regions are proximal to active terrestrial glaciers, which may play a significant role in delivering reactive Fe and Mn to the marginal environments (Raiswell et al., 2018; Wehrmann et al., 2014). The disproportionate importance of Arctic shelves and margins on ocean biogeochemistry indicates that changes in benthic cycling of carbon, trace metals, and nutrients associated with warming in the Arctic will have significant effects on regional and even global, biogeochemical cycles (Macdonald et al., 2015).

Here, we investigate Fe and Mn cycling on the Yermak Plateau and Barents Sea slope that separate the archipelago of Svalbard from the deep Eurasian basin. The goal of this paper is to evaluate whether continental margin sediments act as an important source of Fe and Mn to Arctic bottom waters. We use paired sediment and pore water geochemistry on multicores to investigate spatial and downcore patterns of Fe and Mn cycling in nine locations spanning the northern Svalbard continental slope, the Sophia Basin, and the Yermak Plateau. These results are paired with total organic carbon and Chlorophyll *a* data to investigate the coupling of surface productivity with remobilization of metals within sediments. In response to modern climate change, sea ice coverage, patterns of surface productivity, and fluxes of labile carbon are all changing in the Arctic region. Due to the important links between organic carbon delivery to the seafloor and the fate of Fe and Mn, current and future environmental conditions in the Arctic are evaluated to determine whether the role of continental margins in Fe and Mn cycling is likely to change in response to future climate change.

2. Study Site

The study focuses on the continental margin of the Eurasian Basin, north of Svalbard and the Barents Sea (Figure 1). North of the Barents Sea slope, the Yermak Plateau is a bathymetric feature off the northwestern coast of Svalbard, at the entrance of the Arctic Ocean. To the east, the Yermak Plateau is separated from the Barents Sea slope by the deep Sophia Basin (Sofia Deep). Modern sedimentation rates are generally low and similar in both the northern Barents Sea and the Yermak Plateau. The modern sedimentation rate in the Barents Sea northeast of Svalbard, including the Barents Sea slope, ranges from 0.5–1.0 mm/yr (Nickel et al., 2008), and the modern sedimentation rate on the Yermak Plateau was determined to be 0.7 mm/yr (Howe et al., 2008).

The Eurasian margin region is covered by sea ice during the winter, and during the summer, it is positioned within the marginal sea ice zone, which is the transition between the open ocean and sea ice. New sea ice forms during autumn and winter months, with the sea ice maximum occurring in March. At this time, Svalbard is generally enclosed by ice. Sea ice melt begins in March, with a minimum extent generally

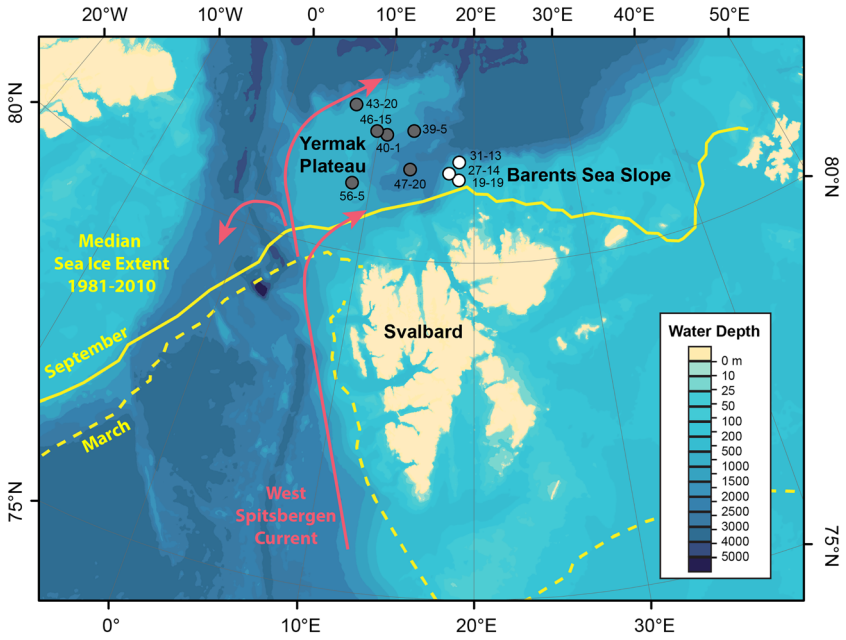

Figure 1. Map of the Barents Sea and Eurasian Arctic margin including Barents Sea slope (white), Sofia Basin (gray), and Yermak Plateau (gray) cores. The median March (dashed) and September (solid) sea ice extent from 1981 to 2010 is indicated in yellow (data from National Snow and Ice Data Center, https://www.nsidc.org). The West Spitsbergen Current is indicated in red. Bathymetry is indicated by shades of blue (Jakobsson et al., 2012).

reached in September. Recent sea ice loss in the Barents Sea is consistent with increasingly warmer ocean conditions and "Atlantification" of this part of the Arctic Ocean (Årthun et al., 2012; Barton et al., 2018). Winter sea ice loss, or the lack of new sea ice formation, in the Barents Sea region is particularly significant compared to other Arctic regions (Onarheim et al., 2018).

To the west of Svalbard, the West Spitsbergen Current delivers nutrient-rich, warm, saline, Atlantic water into the Arctic (Figure 1). In the Fram Strait, between 78° and 80° N, the West Spitsbergen Current splits into multiple branches. Some water recirculates through the Fram Strait and returns southward (Hattermann et al., 2016; von Appen et al., 2016). The largest branch, the Svalbard Current, follows the western and then northern continental margin of Svalbard, before following the eastern continental margin of the Eurasian Basin (Aagaard et al., 1987; Coachman & Aagaard, 1974; Cokelet et al., 2008; Muench et al., 1992; Sirevaag et al., 2011). The Yermak Branch follows the western flank of the Yermak Plateau (Manley, 1995; Manley et al., 1992), and another branch flows through the Yermak Pass (Koenig et al., 2017).

Table 1
Locations of Cores in This Study

Core	Water depth (m)	Latitude	Longitude
Barents Sea slope			
PS92/019-19-MC	481	81° 13.79′ N	18° 33.04′ E
PS92/027-15-MC	795	81° 19.55′ N	17° 16.87′ E
PS92/031-13-MC	1852	81° 30.20′ N	18° 31.72′ E
Sophia Basin			
PS92/047-20-MC	2,175	81° 20.68′ N	13° 39.94′ E
Yermak Plateau (eastern flank)			
PS92/039-05-MC	1,523	81° 55.50′ N	13° 37.98′ E
PS92/040-01-MC	1,158	81° 49.04′ N	10° 52.06′ E
PS92/046-15-MC	886	81° 50.62′ N	09° 45.48′ E
PS92/056-05-MC	854	81° 0.94′ N	08° 17.05′ E
Yermak Plateau (western flank)			
PS92/043-20-MC	817	82° 10.45′ N	07° 0.53′ E

Note. Full site names are given here and shortened in the text to the station name (i.e., for the first core in the Table 19) and deployment number (i.e., for the first core in the Table 19).

3. Methods and Materials

Samples were retrieved from the icebreaker RV *Polarstern* during the Transitions in the Seasonal Sea Ice Zone expedition (PS92) in spring 2015 (Peeken, 2016; Figure 1). Sediment cores were taken using a multicorer at nine locations (Table 1 and Figure 1). Pore water pH was measured at 1 cm intervals onboard using a punch-in pH electrode. Cores were sliced shipboard at 1 cm resolution; slices were frozen at −20°C and subsequently freeze dried.

The studied cores were sampled at sea; however, gravity and kastenlot cores collected nearby were returned to shore intact, and digital photos from the upper 40–50 cm are included in Figure 2. On the deep Barents Sea slope (28-GC) and Yermak Plateau

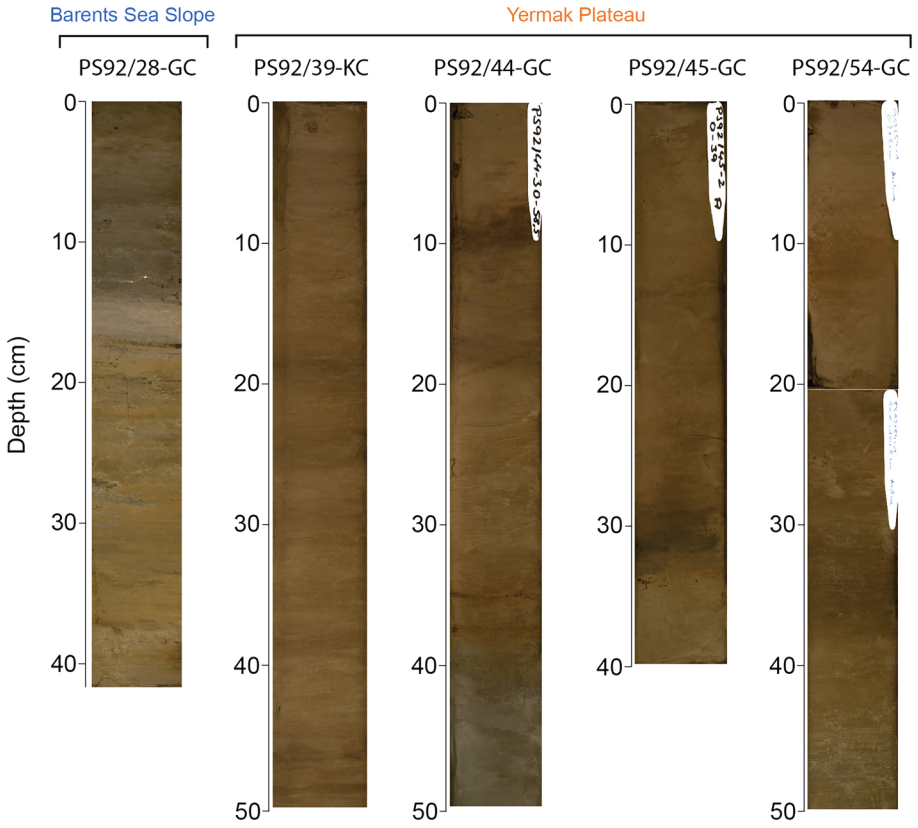

Figure 2. Digital images of the upper 40–50 cm of kastenlot and gravity cores from the study area, including the Barents Sea slope (28-GC) and the Yermak Plateau (39-KC, 44-GC, 46-GC, and 54-GC).

(39-KC, 44-GC, 45-GC, and 54-GC), gravity cores were retrieved close enough to multicore sites for comparison. No gravity cores were collected on the shallow Barents Sea slope or Sophia Basin. Chronology from Yermak Plateau gravity and kastenlot cores indicate that the Holocene begins below 60 cm (Wiers et al., 2019), supporting that the studied sediments are Holocene in age. No chronology exists for the Barents Sea slope cores.

Freeze-dried samples were powdered with an agate mortar and pestle, fused into borate glass beads, and analyzed using wavelength-dispersive X-ray fluorescence with a Philips PW-2400 wavelength-dispersive X-ray fluorescence spectrometer calibrated with 53 geostandards at the University of Oldenburg (for detailed method description, see Eckert et al., 2013). Full downcore profiles were produced on five cores (PS92/19-19, 27-15, 39-5, 46-15, and 56-5). Results for Fe and Mn are presented as Fe/Al and Mn/Al ratios to normalize for variability in detrital input and to allow values to be compared to average shale values. The choice of normalization does not affect the overall trends in the data. Nonnormalized Fe and Mn results are plotted in supporting information Figure S1.

Sequential Fe extractions were adapted from Poulton and Canfield (2005) and Raiswell et al. (2010) to quantify highly reactive Fe phases (Fe_{HR}), that is, phases with half-lives of less than a year when exposed to hydrogen sulfide (Poulton et al., 2004). These are the phases that are typically dissolved in the dissimilatory iron reduction pathway during organic matter degradation. Within the Fe_{HR} pool, poorly crystalline Fe oxyhydroxides (Fe_{ox1}) were extracted using a 24 hr ascorbic acid solution buffered at pH 7.5 (Raiswell et al., 2010). Carbonate-associated Fe (Fe_{carb}) was extracted with sodium acetate (pH 4.5) for 48 hr at 50°C. Crystalline Fe (oxyhydr)oxides (Fe_{ox2}) were extracted by citrate-buffered Na-dithionite (pH 4.8) for 2 hr, and magnetite Fe (Fe_{mag}) was extracted by ammonium oxalate (pH 3.2) for 6 hr. Reactive Mn (Mn_{react}) phases were extracted using citrate-Na dithionite solution buffered with bicarbonate to pH of 7.6 for 8 hr (Ruttenberg, 1992; van der Zee & van Raaphorst, 2004).

Carbon concentrations were measured on a LECO CS244 carbon analyzer at the University of Newcastle. Total organic and inorganic carbon were determined using paired acidified (organic) and unacidified (total) carbon measurements. In preparation for analysis of total organic carbon, samples were acidified in 5% HCl until all the carbonate was removed. Dried samples were powdered and homogenized in an agate mortar and pestle. Pigment concentrations were analyzed fluorometrically following methods described in Holm-Hansen et al. (1965) to determine Chl *a* concentrations. About 1 g of dried sediment was extracted with 10 ml of 90% acetone at 4°C in the dark. After 24 hr, sediment was then centrifuged (3,000 rpm for 2 min) and analyzed using a Turner Designs AU-10 fluorometer before and after acidification with 100 μl 0.3 M HCl. Results for most study locations are previously published in Oleszczuk et al. (2019) and Tessin et al. (2020).

Pore waters were extracted from a separate multicore retrieved from the same deployment onboard using Rhizon samplers (Rhizosphere; 0.15 μm pore size) with vacuum applied by plastic syringes with wooden stoppers (Seeberg-Elverfeldt et al., 2005). Samples were collected at resolutions between 1 and 5 cm, with decreasing resolution downcore. Pore waters were acidified with ultrapure HCl and stored at 4°C. Pore waters were then analyzed for major element composition by inductively coupled plasma-optical emission spectrometry (Thermo iCAP 7400 ICP-OES) at the University of Leeds. Ammonium (NH_4^+) was analyzed onboard, on diluted samples, using a Turner Design Trilogy fluorometer following the method of Holmes et al. (1999).

4. Results

4.1. Bulk Sedimentary Geochemistry

Sediments in the study area are dominated by sand and mud with variable amounts of gravel (Oleszczuk et al., 2019; Stein et al., 1994). Geochemical proxies for grain size and lithogenic source (Al/Ti ratios) in sediments are relatively stable across sites and with depth (15.2–16.9; Supporting Information S1) suggesting generally stable sediment composition. Core 27-15 is an exception with a wider range of Al/Ti values (14.6–18.8). Core photos from 28-GC support the variable sedimentology at this site, as there is a distinct sedimentological shift in the core that is consistent with a shift in sediment geochemistry (Figure 2).

In general, Fe and Mn are more enriched in the Yermak Plateau sediments (39-5, 46-15, and 56-5) than at the slope sites (19-19 and 27-15; Figure 3). Within the analyzed samples, Mn contents range from 0.029% to 1.15%, with Mn/Al ratios of between 0.004 and 0.16 (Figure 3). The Fe contents range from 2.54% to 5.57% with Fe/Al ratios of 0.48 to 0.77 (Figure 3). Downcore records from the slope sites highlight enrichments in Mn/Al in the upper ~5 cm. This is especially noteworthy in Core 19-19, which has a significant Mn/Al peak of 0.046% as compared to deeper Mn/Al values, which average 0.0048%. Sediments from the Yermak Plateau exhibit either constant downcore concentrations or enrichments in Mn at greater depth (>15 cm).

Patterns of Fe/Al are similar to Mn/Al, with the lowest Fe/Al values measured on the Barents Sea slope (0.48). The Yermak Plateau cores exhibit elevated values (average of 0.61). Most of the cores have relatively constant Fe/Al values downcore, with the exception of a significant subsurface peak in Fe/Al in Core 19-19, from the uppermost continental slope (Figure 1). This Fe/Al peak of 0.77 is only 1.5 times larger than the baseline values, whereas the subsurface peak in Mn/Al from the same core is an order of magnitude larger than baseline values.

Figure 4 illustrates differences in Mn/Al values between cores. In general, the two slope sites exhibit Mn/Al values similar to or below the average shale value of 0.0096, while the Yermak Plateau sites are significantly enriched in Mn compared to this value. The exceptions to this pattern are Core 19-19 samples from within the shallow subsurface Mn peak. Similar patterns are apparent in Fe/Al; however, the differences appear less distinct due to the larger absolute ranges in Fe concentrations (Figure 4). Specifically, the majority of slope site samples have Fe/Al values less than the average shale value of 0.55, with the noted exception of the subsurface layer in Core 19-19 that shows a marked enrichment in Fe. Similar to Mn, most of the Yermak Plateau data indicate Fe contents greater than the average shale value.

Concentrations of TOC in the surface sediments (0–0.5 cm) range from 0.53% to 1.61%. No clear trends exist based on water depth or region (Table 2). Chl *a* concentrations in the surface sediments (0–2 cm) range from 0.04 and 0.71 μg/g (Table 2). Barents Sea slope surface sediments have an average of 0.54 μg/g Chl *a*, and Yermak Plateau and Sofia Basin surface sediments have an average of 0.08 μg/g.

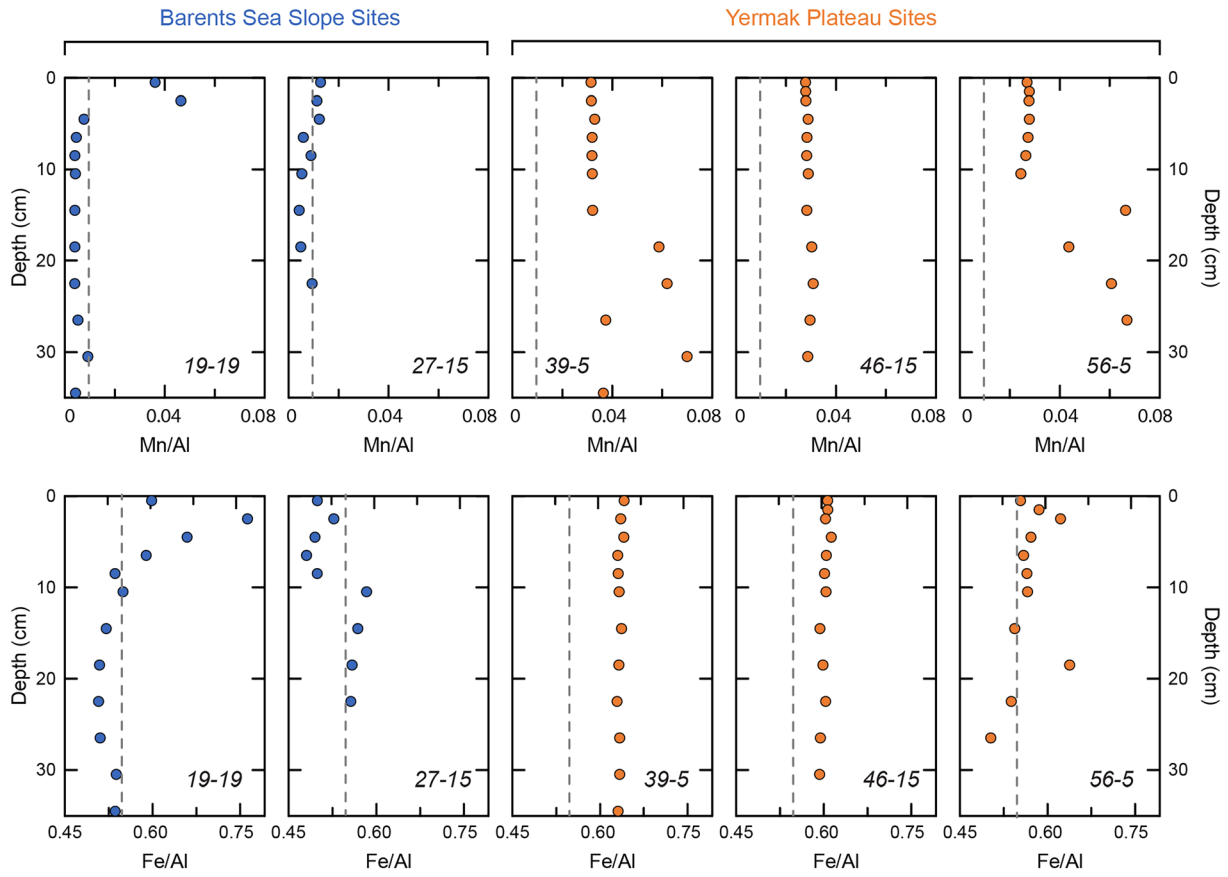

Figure 3. Representative downcore Fe/Al and Mn/Al records from the northern Barents Sea slope (blue) and the Yermak Plateau (orange). Dashed lines indicate the average shale ratios of Mn/Al (0.0096) and Fe/Al (0.55).

4.2. Reactive Sedimentary Fe and Mn Phases

Results from Fe and Mn extractions are presented in Table 2. In general, contents of reactive Fe and Mn phases are the lowest in Barents Sea slope cores, with the exception of near-surface (0–5 cm) sediments from Core 19-19, which exhibit the highest contents of these phases. Sophia Basin and Yermak Plateau cores

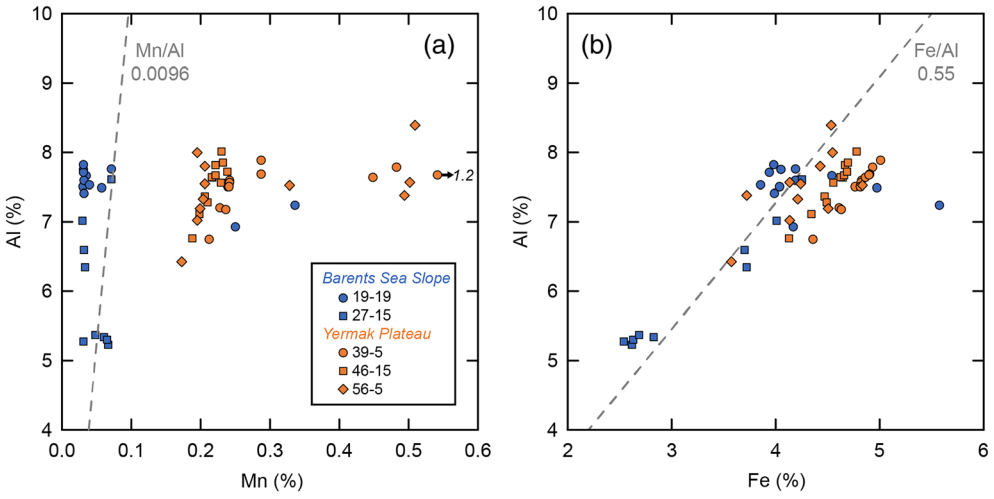

Figure 4. Cross-plots of (a) Mn and (b) Fe versus Al from the northern Barents Sea slope (blue) and the Yermak Plateau (orange). Dashed lines indicate the average shale ratios of Mn/Al (0.0096) and Fe/Al (0.55).

Table 2
Concentrations of Reactive Fe and Mn Phases (wt. %), Total Organic Carbon (TOC; wt. %) in Surface (0–0.5 cm), and Chl a (μg/g) in Surface Sediments (0–2 cm)

Core	Fe_{ox1}	Fe_{HR}	Mn_{react}	$TOC_{0–0.5}$	Chl $a_{0–2}$
Barents Sea slope					
19-19 (<5 cm)	0.35	2.73	0.0219	1.61	0.71
19-19 (>5 cm)	0.06	1.80	0.0038		
27-15	0.07	1.28	0.0045	0.90	0.64
31-13	0.04	0.99	0.0031	0.53	0.27
Sofia Basin					
47-15	0.29	2.19	0.0075	1.24	0.10
Yermak Plateau (eastern flank)					
39-5	0.23	2.03	0.0071	1.24	0.09
40-1	0.22	1.92	0.0073	0.64	
46-15	0.21	1.94	0.0066	1.12	0.08
56-5	0.20	1.91	0.0065	0.84	
Yermak Plateau (western flank)					
43-20	0.13	1.55	0.0061	0.65	0.04

exhibit elevated contents of these phases with the highest values found in the Sophia Basin and the lowest found on the northwestern flank of the Yermak Plateau. Of note, higher contents of reactive Fe and Mn phases are not clearly correlated to water depth. Rather than Fe and Mn being enriched in deep sites as compared to shallow sites, the shallower sites (i.e., 46-15 and 56-5; ~800–900 m) on the Yermak Plateau contain significantly more reactive Fe and Mn, while the deep slope site (31-13; 1,852 m) has the lowest concentrations of these phases (Figure 5).

4.3. Pore Water Chemistry

Dissolved pore water Fe and Mn concentrations are relatively high (~20–150 and ~20–40 μmol, respectively) at the slope sites (19-19 and 31-13) below 2 cm depth in the sediments (Figure 6). Sites 39-5 and 40-1 on the Yermak Plateau both exhibit large increases in porewater Mn (>100 μmol) below ~15 cm sediment depth, while Site 46-5 shows no elevated dissolved Mn concentrations. Dissolved Fe on the Yermak Plateau sites is consistently below 10 μmol and below detection limit for most samples. Dissolved total sulfur profiles are generally flat downcore with values ranging from 24 to 30 mmol (Figure 6).

At the slope sites (19-19 and 31-13), pore water NH_4^+ increases below the sediment-water interface downcore to values of ~65 and ~16 μmol, respectively (Figure 6). At two Yermak Plateau sites (39-5 and 40-1), NH_4^+ increases below ~20 cm depth in the sediment to ~15 and ~8 μmol, respectively. At 46-15, pore water NH_4^+ is similar to bottom water values.

The pH of the bottom water ranged from 7.87 to 8.03 (Figure 7). The pH decreases below the sediment water interface at each location. In Cores 19-19 and 27-15, the pH decreases to minimum values at 3.5 cm (7.13 and 7.24, respectively) before increasing again below this depth. In the Yermak Plateau sites, the pH decreases within the upper 5 cm before stabilizing to minimum values of 7.40–7.46.

5. Discussion

Porewater profiles of Fe, Mn, and NH_4^+ indicate distinct sedimentary redox conditions on the Barents Sea slope as compared to the Yermak Plateau and Sofia Basin (Figure 6). In all cores, Fe, Mn, and NH_4^+ are not present in porewaters within the surface 2 cm, indicating that the surface sediments are oxic in all locations. While macrofaunal and megafaunal activity in these benthic environments may help maintain the

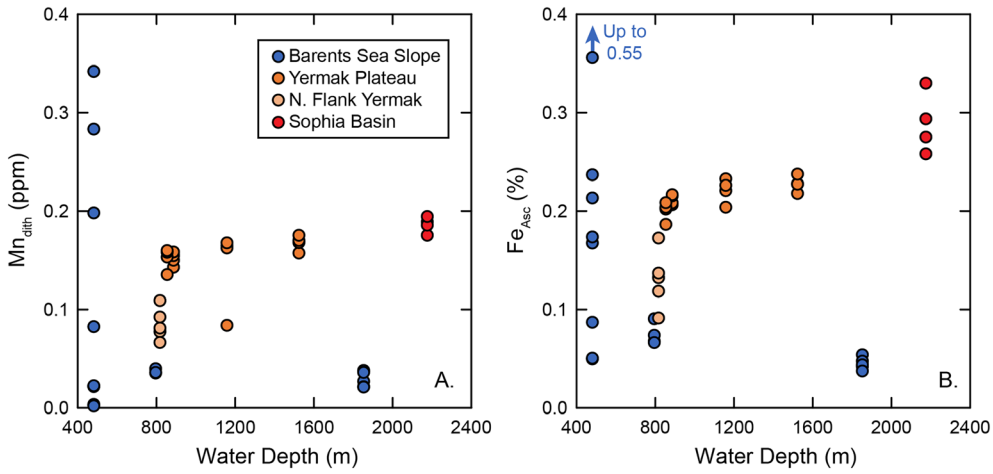

Figure 5. Concentrations of the most reactive (a) Mn (dithionite extractable) and (b) Fe (ascorbic acid extractable) versus water depth of the northern Barents Sea slope (blue) and the Yermak Plateau (orange).

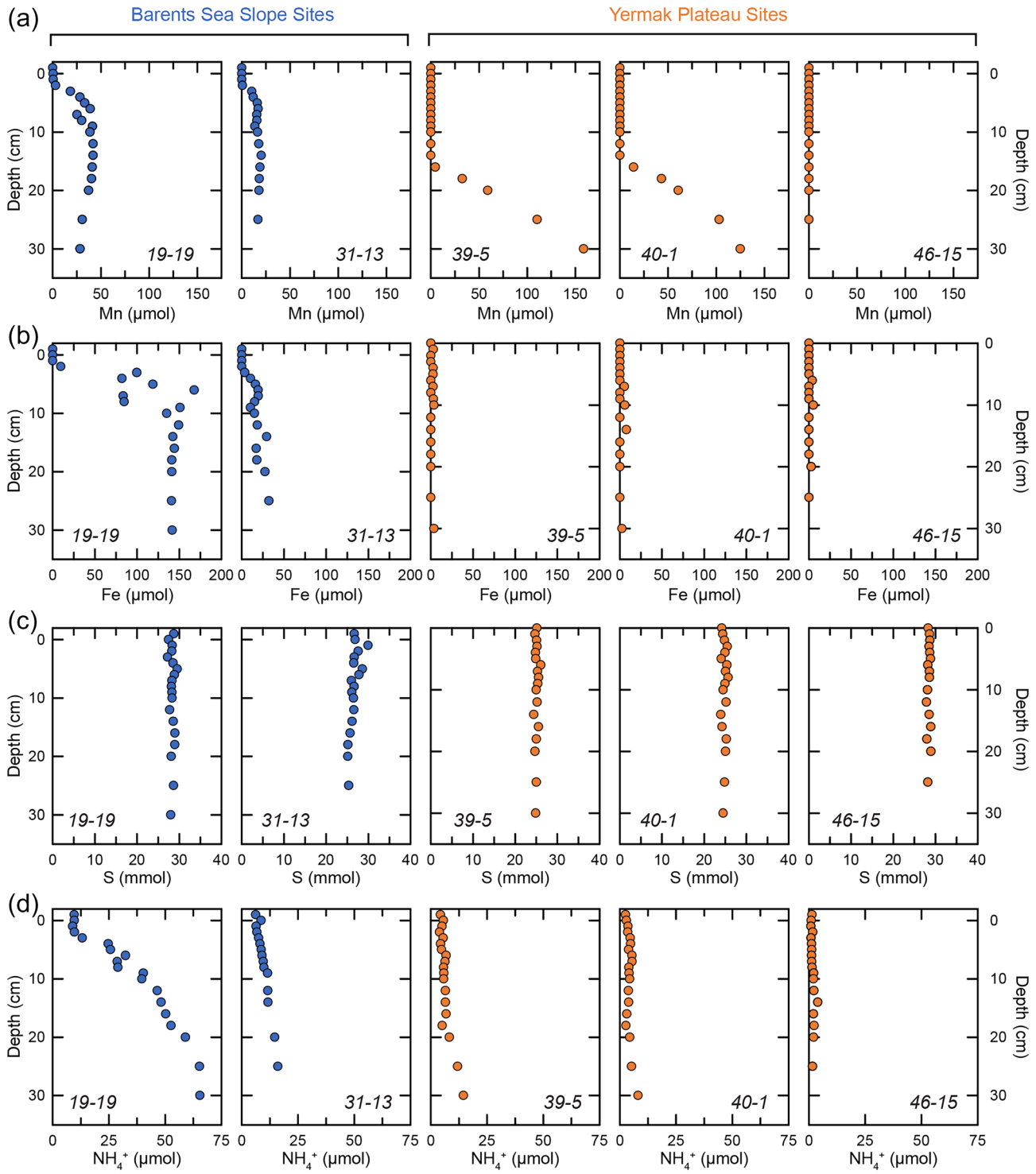

Figure 6. Representative downcore records of pore water chemistry (a) Mn, (b) Fe, (c) total S, and (d) NH4+ from the northern Barents Sea slope (blue) and the Yermak Plateau (orange).

oxygenated surface sediments, bioturbation rates at these core sites are low, and biodiffusion was immeasureable (Oleszcuk et al., 2019).

On the Barents Sea slope, significant Fe and Mn release into the pore waters below the surface sediments, coeval with an increase in pore water NH_4^+, indicates a shift from oxic respiration to Fe and Mn

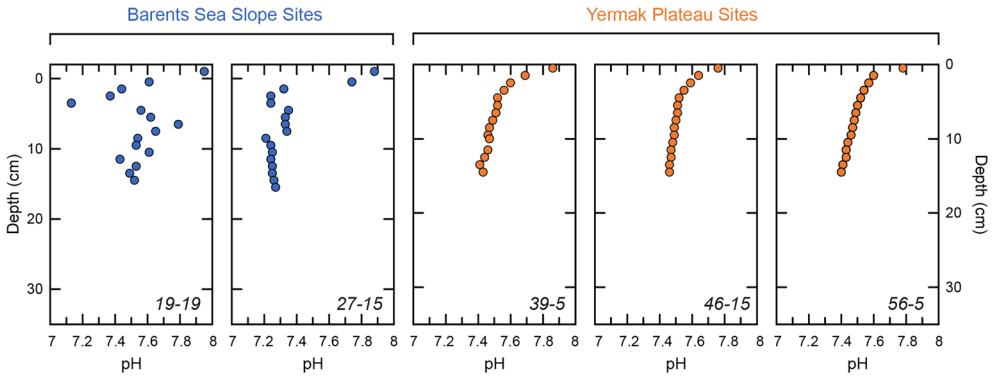

Figure 7. Representative downcore records of pH from the northern Barents Sea slope (blue) and the Yermak Plateau (orange).

reduction as the dominant metabolic pathways of organic carbon remineralization. Conversely, sediment cores from the Sofia Basin and Yermak Plateau exhibit no pore water enrichments in Fe, Mn, or NH_4^+ within the upper 15 cm, suggesting that the oxidant demand within these sediments is lower. However, in two Yermak Plateau cores (39-5 and 40-1), Mn concentrations in porewaters are much higher where Mn reduction occurs below 15 cm. Porewater S profiles are generally flat within all cores, indicating that sulfate reduction is not a dominant metabolic process (Figure 6). If significant sulfate reduction did occur within the sediments, S drawdown would be expected as HS^- reacted with Fe to form solid Fe sulfides.

The difference in oxidant demands between the Barents Sea slope and the Yermak Plateau is likely controlled by differences in the flux of labile organic carbon to the seafloor. Chl *a* results indicate that the Barents Sea slope receives a higher flux of labile organic carbon. Concentrations of Chl *a* can be used as an indicator of the input of labile organic matter (Bourgeois et al., 2017) and tend to be strongly correlated to sediment oxidant demand (Renaud et al., 2008). The highest concentrations of Chl *a* are found on the Barents Sea slope (Table 2), supporting the higher flux of labile organic carbon to these sites, as compared to the Yermak Plateau. Conversely, TOC values are not consistently higher on the Barents Sea slope, as compared to the Yermak Plateau. In general, sedimentary organic carbon concentrations are high near the Eurasian Arctic, despite generally low production and preservation of marine organic carbon due to a supply of terrigenous organic matter (Stein et al., 1994). Since these organic carbon sources are likely to be less labile than fresh marine organic carbon, TOC is unlikely to be an appropriate proxy for oxidant demand. Chl *a* results are broadly in agreement with previous work that suggested increased preservation of marine organic matter along the Svalbard shelf and slope, as compared to the Yermak Plateau and Arctic basins, coincident with reduced sea ice cover and increased nutrient supply from the West Spitsbergen current (Stein et al., 1994).

Higher labile carbon availability and sedimentary oxidant demand on the Barents Sea slope are supported by porewater pH data (Figure 7). Organic matter oxidation lowers pH (Soetaert et al., 2007). Lower minimum pH values (7.13–7.24) were measured in Barents Sea slope cores, as compared to Yermak Plateau and Sofia Basic cores (7.40–7.46). Within Core 19-19, a clear transition from decreasing to increasing pH values can be seen at 3 cm, which is indicative of a shift from oxic remineralization of organic matter, which lowers pH values, to Fe and Mn reduction, which increases pH values (Soetaert et al., 2007).

Differences in the oxidant demand between regions likely control the observed patterns of Fe and Mn remobilization. Within the Arctic Ocean, specifically, the repeated process of metal oxide dissolution-reprecipitation has been well documented as an important component of the Mn cycle (Macdonald & Gobeil, 2012). Generally in the Arctic, Mn redistribution from shallow continental shelf and margin sites (<1,000 m) to the deeper basins has been observed. The same process has been proposed to affect the distribution of Fe from Arctic shelves/margins to the deep basins (März et al., 2012; Meinhardt et al., 2016).

In Core 19-19 from the shallow Barents Sea slope, reprecipitation of Fe and Mn (oxyhydr)oxides produces near-surface enrichments in Fe and Mn (Figure 2). The most easily reducible Fe and Mn phases are reduced

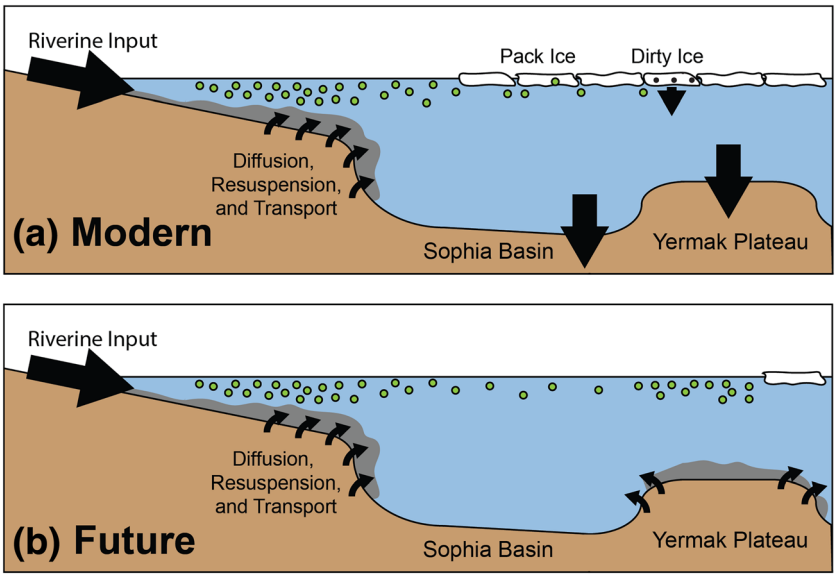

Figure 8. Cartoon depicting (a) the modern transport and remobilization of Fe and Mn from the northern Barents Sea slope to the Sofia Basin and Yermak Plateau and (b) the proposed future conditions with higher organic matter export.

within deeper sediments, Fe^{2+} and Mn^{2+} diffuse into oxic surface sediments, and Fe and Mn (oxyhydr)oxides precipitate just below the sediment-water interface. In both 19-19 and 31-13, further evidence of this process can be seen in the pore water geochemistry (Figure 6). While reactive Fe and Mn on the shallow Barents Sea slope is currently trapped in the near-surface sediments, the accumulation of these mineral phases near the seafloor makes them susceptible to physical or biogeochemical remobilization into the water column. In the third Barents Sea slope core (27-15), Fe and Mn are depleted throughout the entire core, including the surface sediments. Fe and Mn were likely remobilized to the surface and near-surface layers and subsequently lost to the water column. This core is located on a steeper slope, which may be more susceptible to sediment transport and physical resuspension of Fe- and Mn-rich surface sediments.

On the Yermak Plateau and Sofia Basin, early diagenetic Fe and Mn reduction does not occur within near-surface sediments, allowing reactive Fe and Mn phases to accumulate within the uppermost 30–50 cm of the sedimentary column. The core images illustrate that the Yermak Plateau sediments are consistently red-brown in color due to the high concentrations of reactive Fe and Mn (Figure 2). Conversely, the upper 15 cm of sediments from the Barents Sea slope are grayer, due to lower concentrations of Fe and Mn. Although no core image is available for the shallow Barents Sea slope near Core 19-19, individual sample descriptions are consistent with sediments similar to the upper 15 cm of sediments on the deep slope but with distinct orange-brown sediments in the upper 5 cm of the core, due to elevated concentrations of Fe and Mn.

The inventory of reactive Fe and Mn phases on the Yermak Plateau is susceptible to remobilization if the oxidant demand increases in these regions. The high concentrations of porewater Mn in Yermak Plateau cores highlight the potential for significant remobilization of Fe and Mn within these locations if the redoxcline shifts upward in the sediments in response to an increased oxidant demand.

6. Implications

While these new results are consistent with processes discussed in previous Arctic sediment geochemical studies, namely, that Fe and Mn are shuttled away from sediments underlying more productive regions to less productive regions (Macdonald & Gobeil, 2012; März et al., 2012; Meinhardt et al., 2016), the physiographic distribution of sampling stations is unique and has significant implications. In particular, the pattern of Fe and Mn loss from the sediments is not indicative of shuttling from shallow to deep sites but rather from productive marginal ice regions to perennially ice-covered regions (Figure 5). Since primary productivity and

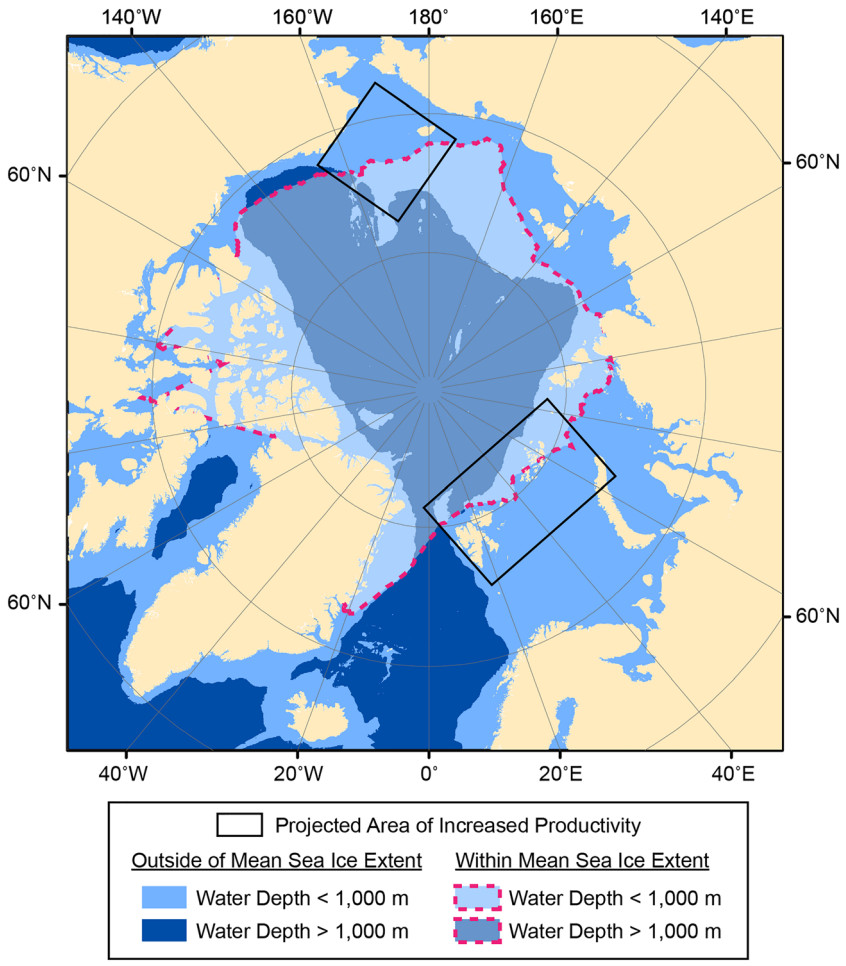

Figure 9. Map of the Arctic Ocean. Minimum sea ice cover (September) is indicated by white shading (NSIDC). Water depths less than 1,000 m are indicated by lighter blue shades. Regions that are expected to experience increased primary productivity are indicated by black boxes. These regions represent areas of agreement between multiple projections (Slagstad et al., 2015; Vancoppenolle et al., 2013).

sea ice extent in this region are both very sensitive to climate change, the link between patterns of Fe and Mn remobilization and these factors highlights that Fe and Mn cycling is likely to change in response to future climate change.

Climatically sensitive, sedimentary inventories of reactive Fe and Mn in shallow sites are particularly important because they comprise a potential source of Fe and Mn to the water column (Figure 8). Including the Yermak Plateau, large regions of the Arctic continental margins are currently perennially ice covered (Figure 9). Because Fe and Mn minerals play an important role in organic carbon, nutrient and trace metal cycling, reduction, and redistribution of easily reducible mineral phases from these relatively shallow sites would affect not only the Fe and Mn cycles but also organic carbon, nutrient, and trace metal cycles. While deep basin and abyssal plain sediments could become a source of Fe and Mn as well, they are unlikely to be as important as margin settings, such as the Yermak Plateau. Deep basin sediments are likely to remain organic poor because organic material is likely to remineralize within the deeper water column before reaching the seafloor. Additionally, benthic fluxes of micronutrients and macronutrients from shallow sites are more likely to be returned to the photic zone, where they might impact primary productivity.

In order for the Yermak Plateau and other shallow, historically perennially ice-covered regions to become sources of Fe and Mn, productivity would need to increase in the overlying waters. Sea ice is thinning in the Eurasian Arctic (Renner et al., 2014), and ice-free summers over the Yermak Plateau are becoming

more common (e.g., DeRepentigny et al., 2016). As Arctic sea ice continues to retreat, seasonally ice-free conditions on the Yermak Plateau are expected to become more common. Additionally, increased influence of Atlantic water in this region, due to a stronger West Spitsbergen current, will increase nutrient availability in this region (e.g., Wang et al., 2020). These changes will likely lead to shifts in surface water productivity, with models suggesting that the largest increases in primary productivity in the Arctic Ocean will occur on the Eurasian perimeter, including the northern Barents Sea (Slagstad et al., 2015; Vancoppenolle et al., 2013). These studies also agree on areas of the Chukchi Sea as loci of future productivity increases (Figure 9). Current trends in productivity indicate that the Barents Sea and Eurasian Arctic are experiencing the most rapid increase in Chl *a* derived primary productivity (Frey et al., 2019) within the Arctic Ocean.

If current trends continue and future projections prove correct, the marginal sea ice zone and locus of surface productivity will shift northward, leading to enhanced organic carbon export to the seafloor. The resulting increased oxidant demand within Yermak Plateau sediments will ultimately lead to reactive Fe and Mn phases becoming more important for near-surface organic carbon oxidation. Our results from Yermak cores indicate deep (>15 cm) reduction of Mn (oxyhydr)oxides and release of dissolved Mn into pore waters (Figure 6). These sizeable deeper pore water Mn enrichments suggest that as oxidant demand in sediments increases and the redoxcline shoals within sediments, Mn (oxyhydr)oxides can be easily reduced. This will result in Fe and Mn accumulations within near-surface sediments, where these minerals are poised for physical or biogeochemical remobilization into the water column, where Fe, in particular, may be returned to the photic zone to fuel further primary productivity.

7. Conclusions

Sediment and pore water records from the Eurasian margin north of Svalbard allow for the examination of regional patterns of Fe and Mn cycling and transport. Manganese is remobilized in the Barents Sea slope cores, producing near-surface enrichment layers and depletions downcore. Iron follows a similar trend in these cores, with deeper reduction of Fe (oxyhydr)oxides and diffusion/reprecipitation of Fe (oxyhydr)oxides in near-surface sediment layers. In contrast, cores from the Yermak Plateau and Sofia Basin exhibit enrichments in reactive Fe and Mn phases throughout the sediment cores, suggesting that a low oxidant demand due to low organic carbon flux leads to these mineral phases accumulating at all sediment depths.

The geographic pattern of remobilization is an especially important result of this work. Unlike previous work, which has documented Mn shuttling from shelves to deep basins (Macdonald & Gobeil, 2012; März et al., 2012), this work documents Mn and Fe shuttling from the Barents Sea slope to the Yermak Plateau and Sofia Basin independent of water depth. Instead, the regional patterns are best explained by patterns of primary productivity and organic carbon flux, which are controlled by sea ice cover and delivery of nutrient-rich water by the West Spitsbergen current. As sea ice continues to retreat and the Yermak Plateau becomes seasonally ice-free, productivity is expected to increase. This increase in productivity would increase the flux of organic carbon to the sediments, thereby increasing oxidant demand, and eventually the reduction of Fe and Mn mineral phases. These findings mean that with reductions in the perennial sea ice cover of the Arctic Ocean, the Yermak Plateau may become a source of Fe, Mn, and associated trace metals to overlying water. In addition to the Yermak Plateau, other submarine plateaus, including Chukchi, Morris Jessup, Mendeleev, and Lomonosov Ridges, have the potential to become sources of benthic redox sensitive metals.

Acknowledgments

The TRANSSIZ cruise (Transitions in the Arctic Seasonal Sea Ice Zone; PS92; Grant AWI_PS92_00) was initiated and co-organized by the Arctic in Rapid Transition (ART) network. The authors thank the crew of RV Polarstern and chief scientist Ilka Peeken. A. T. received funding for this project from the European Union's Horizon 2020 research and innovation programme under the Marie Skłodowska-Curie Grant Agreement 709175. We would like to thank Andy Connelly and Stephen Reid for analytical support.

Data Availability Statement

Data presented in this paper will be available on the Pangea website (https://issues.pangaea.de/browse/PDI-24675).

References

Aagaard, K., Foldvik, A., & Hillman, S. R. (1987). The West Spitsbergen Current: Disposition and water mass transformation. *Journal of Geophysical Research*, *92*(C4), 3778. https://doi.org/10.1029/JC092iC04p03778

Aller, R. C. (1990). Bioturbation and manganese cycling in hemipelagic sediments. *Philosophical Transactions of the Royal Society A: Mathematical, Physical and Engineering Sciences*, *331*(1616), 51–68. https://doi.org/10.1098/rsta.1990.0056

Aller, Robert C. (1994). Bioturbation and remineralization of sedimentary organic matter: Effects of redox oscillation. *Chemical Geology*, *114*(3–4), 331–345. https://doi.org/10.1016/0009-2541(94)90062-0

Årthun, M., Eldevik, T., Smedsrud, L. H., Skagseth, Ø., & Ingvaldsen, R. B. (2012). Quantifying the influence of Atlantic heat on Barents Sea ice variability and retreat*. *Journal of Climate*, *25*(13), 4736–4743. https://doi.org/10.1175/JCLI-D-11-00466.1

Barber, A., Brandes, J., Leri, A., Lalonde, K., Balind, K., Wirick, S., et al. (2017). Preservation of organic matter in marine sediments by inner-sphere interactions with reactive iron. *Scientific Reports*, *7*(1), 366. https://doi.org/10.1038/s41598-017-00494-0

Barton, B. I., Lenn, Y.-D., & Lique, C. (2018). Observed atlantification of the Barents Sea causes the polar front to limit the expansion of winter sea ice. *Journal of Physical Oceanography*, *48*(8), 1849–1866. https://doi.org/10.1175/JPO-D-18-0003.1

Berner, R. A. (1973). Phosphate removal from sea water by adsorption on volcanogenic ferric oxides. *Earth and Planetary Science Letters*, *18*(1), 77–86. https://doi.org/10.1016/0012-821X(73)90037-X

Bourgeois, S., Archambault, P., & Witte, U. (2017). Organic matter remineralization in marine sediments: A Pan-Arctic synthesis. *Global Biogeochemical Cycles*, *31*, 190–213. https://doi.org/10.1002/2016GB005378

Calvert, S., & Pedersen, T. (1993). Geochemistry of recent oxic and anoxic marine sediments: Implications for the geological record. *Marine Geology*, *113*(1–2), 67–88. https://doi.org/10.1016/0025-3227(93)90150-T

Calvert, S. E., & Price, N. B. (1977). Chapter 3 shallow water, continental margin and lacustrine nodules: Distribution and geochemistry (pp. 45–86). https://doi.org/10.1016/S0422-9894(08)71017-1

Coachman, L. K., & Aagaard, K. (1974). Physical oceanography of Arctic and subarctic seas. In *Marine geology and oceanography of the Arctic seas* (pp. 1–72). Berlin, Heidelberg: Springer Berlin Heidelberg. https://doi.org/10.1007/978-3-642-87411-6_1

Coale, K. H., Johnson, K. S., Fitzwater, S. E., Blain, S. P. G., Stanton, T. P., & Coley, T. L. (1998). IronEx-I, an in situ iron-enrichment experiment: Experimental design, implementation and results. *Deep Sea Research Part II: Topical Studies in Oceanography*, *45*(6), 919–945. https://doi.org/10.1016/S0967-0645(98)00019-8

Cokelet, E. D., Tervalon, N., & Bellingham, J. G. (2008). Hydrography of the West Spitsbergen Current, Svalbard branch: Autumn 2001. *Journal of Geophysical Research*, *113*, C01006. https://doi.org/10.1029/2007JC004150

Cullen, J. J. (1991). Hypotheses to explain high-nutrient conditions in the open sea. *Limnology and Oceanography*, *36*(8), 1578–1599. https://doi.org/10.4319/lo.1991.36.8.1578

DeRepentigny, P., Tremblay, L. B., Newton, R., & Pfirman, S. (2016). Patterns of sea ice retreat in the transition to a seasonally ice-free Arctic. *Journal of Climate*, *29*(19), 6993–7008. https://doi.org/10.1175/JCLI-D-15-0733.1

Eckert, S., Brumsack, H.-J., Severmann, S., Schnetger, B., März, C., & Fröllje, H. (2013). Establishment of euxinic conditions in the Holocene Black Sea. *Geology*, *41*(4), 431–434. https://doi.org/10.1130/G33826.1

Elrod, V. A., Berelson, W. M., Coale, K. H., & Johnson, K. S. (2004). The flux of iron from continental shelf sediments: A missing source for global budgets. *Geophysical Research Letters*, *31*, L12307. https://doi.org/10.1029/2004GL020216

Emerson, S., & Hedges, J. (2003). Sediment diagenesis and benthic flux. In *Treatise on geochemistry* (pp. 293–319). Amsterdam: Elsevier. https://doi.org/10.1016/B0-08-043751-6/06112-0

Estes, E. R., Andeer, P. F., Nordlund, D., Wankel, S. D., & Hansel, C. M. (2017). Biogenic manganese oxides as reservoirs of organic carbon and proteins in terrestrial and marine environments. *Geobiology*, *15*(1), 158–172. https://doi.org/10.1111/gbi.12195

Finney, B., Heath, G. R., & Lyle, M. (1984). Growth rates of manganese-rich nodules at MANOP site H (eastern North Pacific). *Geochimica et Cosmochimica Acta*, *48*(5), 911–919. https://doi.org/10.1016/0016-7037(84)90184-4

Frey, K. E., Comiso, J. C., Cooper, L. W., Grebmeier, J. M., & Stock, L. V. (2019). Arctic Ocean primary productivity: The response of marine algae to climate warming and sea ice decline. In J. Richter-Menge, M. L. Druckenmiller, & M. Jeffries (Eds.), *Arctic Report Card 2019*. http://www.arctic.noaa.gov/Report-Card

Froelich, P. N., Bender, M. L., & Heath, G. R. (1977). Phosphorus accumulation rates in metalliferous sediments on the East Pacific Rise. *Earth and Planetary Science Letters*, *34*(3), 351–359. https://doi.org/10.1016/0012-821X(77)90044-9

Froelich, P. N., Klinkhammer, G. P., Bender, M. L., Luedtke, N. A., Heath, G. R., Cullen, D., et al. (1979). Early oxidation of organic matter in pelagic sediments of the eastern equatorial Atlantic: Suboxic diagenesis. *Geochimica et Cosmochimica Acta*, *43*(7), 1075–1090. https://doi.org/10.1016/0016-7037(79)90095-4

Goldberg, E. D. (1954). Marine geochemistry 1. Chemical scavengers of the sea. *The Journal of Geology*, *62*(3), 249–265. https://doi.org/10.1086/626161

Hattermann, T., Isachsen, P. E., Appen, W., Albretsen, J., & Sundfjord, A. (2016). Eddy-driven recirculation of Atlantic water in Fram Strait. *Geophysical Research Letters*, *43*, 3406–3414. https://doi.org/10.1002/2016GL068323

Holmes, R. M., Aminot, A., Kérouel, R., Hooker, B. A., & Peterson, B. J. (1999). A simple and precise method for measuring ammonium in marine and freshwater ecosystems. *Canadian Journal of Fisheries and Aquatic Sciences*, *56*(10), 1801–1808. https://doi.org/10.1139/f99-128

Holm-Hansen, O., Lorenzen, C. J., Holmes, R. W., & Strickland, J. D. H. (1965). Fluorometric Determination of Chlorophyll. *ICES Journal of Marine Science*, *30*(1), 3–15. https://doi.org/10.1093/icesjms/30.1.3

Howe, J. A., Shimmield, T. M., Harland, R., & Eyles, N. (2008). Late Quaternary contourites and glaciomarine sedimentation in the Fram Strait. *Sedimentology*, *55*, 179–200. https://doi.org/10.1111/j.1365-3091.2007.00897.x

Jakobsson, M., Grantz, A., Kristoffersen, Y., & Macnab, R. (2003). Physiographic provinces of the Arctic Ocean seafloor. *Geological Society of America Bulletin*, *115*(12), 1443. https://doi.org/10.1130/B25216.1

Jakobsson, M., Mayer, L., Coakley, B., Dowdeswell, J. A., Forbes, S., Fridman, B., et al. (2012). The International Bathymetric Chart of the Arctic Ocean (IBCAO) Version 3.0. *Geophysical Research Letters*, *39*, L12609. https://doi.org/10.1029/2012GL052219

Johnson, K., Purvis, G., Lopez-Capel, E., Peacock, C., Gray, N., Wagner, T., et al. (2015). Towards a mechanistic understanding of carbon stabilization in manganese oxides. *Nature Communications*, *6*(1), 7628. https://doi.org/10.1038/ncomms8628

Johnson, K. S., Chavez, F. P., & Friederich, G. E. (1999). Continental-shelf sediment as a primary source of iron for coastal phytoplankton. *Nature*, *398*(6729), 697–700. https://doi.org/10.1038/19511

Johnson, K. S., Coale, K. H., Berelson, W. M., & Michael Gordon, R. (1996). On the formation of the manganese maximum in the oxygen minimum. *Geochimica et Cosmochimica Acta*, *60*(8), 1291–1299. https://doi.org/10.1016/0016-7037(96)00005-1

Johnson, K. S., Gordon, R. M., & Coale, K. H. (1997). What controls dissolved iron concentrations in the world ocean? *Marine Chemistry*, *57*(3–4), 137–161. https://doi.org/10.1016/S0304-4203(97)00043-1

Kaiser, K., & Guggenberger, G. (2000). The role of DOM sorption to mineral surfaces in the preservation of organic matter in soils. *Organic Geochemistry*, *31*(7–8), 711–725. https://doi.org/10.1016/S0146-6380(00)00046-2

Koenig, Z., Provost, C., Sennéchael, N., Garric, G., & Gascard, J.-C. (2017). The Yermak Pass branch: A major pathway for the Atlantic water north of Svalbard? *Journal of Geophysical Research: Oceans*, *122*, 9332–9349. https://doi.org/10.1002/2017JC013271

Kuma, K., Nishioka, J., & Matsunaga, K. (1996). Controls on iron (III) hydroxide solubility in seawater: The influence of pH and natural organic chelators. *Limnology and Oceanography*, *41*(3), 396–407. https://doi.org/10.4319/lo.1996.41.3.0396

Lalonde, K., Mucci, A., Ouellet, A., & Gélinas, Y. (2012). Preservation of organic matter in sediments promoted by iron. *Nature*, *483*(7388), 198–200. https://doi.org/10.1038/nature10855

Lam, P. J., Bishop, J. K. B., Henning, C. C., Marcus, M. A., Waychunas, G. A., & Fung, I. Y. (2006). Wintertime phytoplankton bloom in the subarctic Pacific supported by continental margin iron. *Global Biogeochemical Cycles*, *20*, GB1006. https://doi.org/10.1029/2005GB002557

Liu, K. K., Atkinson, L., Quiñones, R., & Talaue McManus, L. (Eds.) (2010). Biogeochemistry of continental Margins in a global context. In *Carbon and nutrient fluxes in continental margins: A global synthesis*, *The IGBP Series* (pp. 3–24). Springer.

Liu, K.-K., Atkinson, L., Chen, C. T. A., Gao, S., Hall, J., MacDonald, R. W., et al. (2000). Exploring continental margin carbon fluxes on a global scale. *Eos, Transactions American Geophysical Union*, *81*(52), 641. https://doi.org/10.1029/EO081i052p00641-01

Macdonald, R. W., Anderson, L. G., Christensen, J. P., Miller, L. A., Semiletov, I. P., & Stein, R. (2010). The Arctic Ocean. In K.-K. Liu, L. Atkinson, R. Quiñones, & L. Talaue-McManus (Eds.), *Carbon and nutrient fluxes in continental margins* (pp. 291–302). Berlin, Heidelberg: Springer Berlin Heidelberg. https://doi.org/10.1007/978-3-540-92735-8

Macdonald, R. W., & Gobeil, C. (2012). Manganese sources and sinks in the Arctic Ocean with reference to periodic enrichments in basin sediments. *Aquatic Geochemistry*, *18*(6), 565–591. https://doi.org/10.1007/s10498-011-9149-9

Macdonald, R. W., Kuzyk, Z. Z. A., & Johannessen, S. C. (2015). The vulnerability of Arctic shelf sediments to climate change. *Environmental Reviews*, *23*(4), 461–479. https://doi.org/10.1139/er-2015-0040

Manley, T. O. (1995). Branching of Atlantic water within the Greenland-Spitsbergen Passage: An estimate of recirculation. *Journal of Geophysical Research*, *100*(C10), 20627. https://doi.org/10.1029/95JC01251

Manley, T. O., Bourke, R. H., & Hunkins, K. L. (1992). Near-surface circulation over the Yermak plateau in northern Fram Strait. *Journal of Marine Systems*, *3*(1–2), 107–125. https://doi.org/10.1016/0924-7963(92)90033-5

Martin, J. H., & Fitzwater, S. E. (1988). Iron deficiency limits phytoplankton growth in the north-east Pacific subarctic. *Nature*, *331*(6154), 341–343. https://doi.org/10.1038/331341a0

März, C., Poulton, S. W., Brumsack, H.-J., & Wagner, T. (2012). Climate-controlled variability of iron deposition in the Central Arctic Ocean (southern Mendeleev Ridge) over the last 130,000years. *Chemical Geology*, *330-331*, 116–126. https://doi.org/10.1016/j.chemgeo.2012.08.015

McManus, J., Berelson, W. M., Severmann, S., Johnson, K. S., Hammond, D. E., Roy, M., & Coale, K. H. (2012). Benthic manganese fluxes along the Oregon–California continental shelf and slope. *Continental Shelf Research*, *43*, 71–85. https://doi.org/10.1016/j.csr.2012.04.016

Meinhardt, A.-K., März, C., Schuth, S., Lettmann, K. A., Schnetger, B., Wolff, J.-O., & Brumsack, H.-J. (2016). Diagenetic regimes in Arctic Ocean sediments: Implications for sediment geochemistry and core correlation. *Geochimica et Cosmochimica Acta*, *188*, 125–146. https://doi.org/10.1016/j.gca.2016.05.032

Menard, H. W., & Smith, S. M. (1966). Hypsometry of ocean basin provinces. *Journal of Geophysical Research*, *71*(18), 4305–4325. https://doi.org/10.1029/JZ071i018p04305

Moore, C. M., Mills, M. M., Arrigo, K. R., Berman-Frank, I., Bopp, L., Boyd, P. W., et al. (2013). Processes and patterns of oceanic nutrient limitation. *Nature Geoscience*, *6*(9), 701–710. https://doi.org/10.1038/ngeo1765

Muench, R. D., McPhee, M. G., Paulson, C. A., & Morison, J. H. (1992). Winter oceanographic conditions in the Fram Strait-Yermak Plateau region. *Journal of Geophysical Research*, *97*(C3), 3469. https://doi.org/10.1029/91JC03107

Nameroff, T. J., Balistrieri, L. S., & Murray, J. W. (2002). Suboxic trace metal geochemistry in the eastern tropical North Pacific. *Geochimica et Cosmochimica Acta*, *66*(7), 1139–1158. https://doi.org/10.1016/S0016-7037(01)00843-2

Nickel, M., Vandieken, V., Brüchert, V., & Jørgensen, B. B. (2008). Microbial Mn (IV) and Fe (III) reduction in northern Barents Sea sediments under different conditions of ice cover and organic carbon deposition. *Deep Sea Res. Part II Top. Stud. Oceanogr.*, *55*(20-21), 2390–2398. http://doi.org/10.1016/j.dsr2.2008.05.003

Oleszczuk, B., Michaud, E., Morata, N., Renaud, P. E., & Kędra, M. (2019). Benthic macrofaunal bioturbation activities from shelf to deep basin in spring to summer transition in the Arctic Ocean. *Marine Environmental Research*, *150*, 104746. https://doi.org/10.1016/j.marenvres.2019.06.008

Onarheim, I. H., Eldevik, T., Smedsrud, L. H., & Stroeve, J. C. (2018). Seasonal and regional manifestation of Arctic sea ice loss. *Journal of Climate*, *31*(12), 4917–4932. https://doi.org/10.1175/JCLI-D-17-0427.1

Peeken, I. (2016). The Expedition PS92 of the Research Vessel POLARSTERN to the Arctic Ocean in 2015. In *Berichte zur Polar- und Meeresforsch*, *Reports on Polar and Marine Research* (Vol. 694, 153 pp.). https://doi.org.10.2312/BzPM_0694_2016

Poulton, S. W., & Canfield, D. E. (2005). Development of a sequential extraction procedure for iron: Implications for iron partitioning in continentally derived particulates. *Chemical Geology*, *214*(3–4), 209–221. https://doi.org/10.1016/j.chemgeo.2004.09.003

Poulton, S. W., Krom, M. D., & Raiswell, R. (2004). A revised scheme for the reactivity of iron (oxyhydr)oxide minerals towards dissolved sulfide. *Geochimica et Cosmochimica Acta*, *68*(18), 3703–3715. https://doi.org/10.1016/j.gca.2004.03.012

Raiswell, R., Vu, H. P., Brinza, L., & Benning, L. G. (2010). The determination of labile Fe in ferrihydrite by ascorbic acid extraction: Methodology, dissolution kinetics and loss of solubility with age and de-watering. *Chemical Geology*, *278*(1–2), 70–79. https://doi.org/10.1016/j.chemgeo.2010.09.002

Raiswell, R., Hawkings, J., Elsenousy, A., Death, R., Tranter, M., & Wadham, J. (2018). Iron in glacial systems: Speciation, reactivity, freezing behavior, and alteration during transport. *Frontiers in Earth Science*, *6*. https://doi.org/10.3389/feart.2018.00222

Renaud, P. E., Morata, N., Carroll, M. L., Denisenko, S. G., & Reigstad, M. (2008). Pelagic–benthic coupling in the western Barents Sea: Processes and time scales. *Deep Sea Research Part II: Topical Studies in Oceanography*, *55*(20-21), 2372–2380. https://doi.org/10.1016/j.dsr2.2008.05.017

Renner, A. H. H., Gerland, S., Haas, C., Spreen, G., Beckers, J. F., Hansen, E., et al. (2014). Evidence of Arctic sea ice thinning from direct observations. *Geophysical Research Letters*, *41*, 5029–5036. https://doi.org/10.1002/2014GL060369

Rijkenberg, M. J. A., Slagter, H. A., Rutgers van der Loeff, M., van Ooijen, J., & Gerringa, L. J. A. (2018). Dissolved Fe in the deep and upper Arctic Ocean with a focus on Fe limitation in the Nansen Basin. *Frontiers in Marine Science*, *5*(March), 1–14. https://doi.org/10.3389/fmars.2018.00088

Ruttenberg, K. C. (1992). Development of a sequential extraction method for different forms of phosphorus in marine sediments. *Limnology and Oceanography*, *37*(7), 1460–1482. https://doi.org/10.4319/lo.1992.37.7.1460

Seeberg-Elverfeldt, J., Schlüter, M., Feseker, T., & Kölling, M. (2005). Rhizon sampling of porewaters near the sediment-water interface of aquatic systems. *Limnology and Oceanography: Methods*, *3*(8), 361–371. https://doi.org/10.4319/lom.2005.3.361

Sirevaag, A., de la Rosa, S., Fer, I., Nicolaus, M., Tjernström, M., & McPhee, M. G. (2011). Mixing, heat fluxes and heat content evolution of the Arctic Ocean mixed layer. *Ocean Science*, *7*(3), 335–349. https://doi.org/10.5194/os-7-335-2011

Slagstad, D., Wassmann, P. F. J., & Ellingsen, I. (2015). Physical constrains and productivity in the future Arctic Ocean. *Frontiers in Marine Science*, *2*. https://doi.org/10.3389/fmars.2015.00085

Slomp, C. P., Epping, E. H. G., Helder, W., & van Raaphorst, W. (1996). A key role for iron-bound phosphorus in authigenic apatite formation in North Atlantic continental platform sediments. *Journal of Marine Research*, *54*(6), 1179–1205. https://doi.org/10.1357/0022240963213745

Soetaert, K., Hofmann, A. F., Middelburg, J. J., Meysman, F. J. R., & Greenwood, J. (2007). The effect of biogeochemical processes on pH. *Marine Chemistry*, *105*(1-2), 30–51. https://doi.org/10.1016/j.marchem.2006.12.012

Stein, R., & Macdonald, R. W. (2004). Organic carbon budget: Arctic Ocean vs. global ocean. In R. Stein, & R. W. MacDonald (Eds.), *The organic carbon cycle in the Arctic Ocean* (pp. 315–322). Berlin, Heidelberg: Springer Berlin Heidelberg. https://doi.org/10.1007/978-3-642-18912-8_8

Stein, R., Grobe, H., & Wahsner, M. (1994). Organic carbon, carbonate, and clay mineral distributions in eastern central Arctic Ocean surface sediments. *Marine Geology*, *119*(3-4), 269–285. https://doi.org/10.1016/0025-3227(94)90185-6

Tagliabue, A., Bowie, A. R., Boyd, P. W., Buck, K. N., Johnson, K. S., & Saito, M. A. (2017). The integral role of iron in ocean biogeochemistry. *Nature*, *543*(7643), 51–59. https://doi.org/10.1038/nature21058

Taylor, K. G., & Macquaker, J. H. S. (2011). Iron minerals in marine sediments record chemical environments. *Elements*, *7*(2), 113–118. https://doi.org/10.2113/gselements.7.2.113

Tessier, A., Rapin, F., & Carignan, R. (1985). Trace metals in oxic lake sediments: Possible adsorption onto iron oxyhydroxides. *Geochimica et Cosmochimica Acta*, *49*(1), 183–194. https://doi.org/10.1016/0016-7037(85)90203-0

Tessin, A., März, C., Kędra, M., Matthiessen, J., Morata, N., Nairn, M., et al. (2020). Benthic phosphorus cycling within the Eurasian marginal sea ice zone. *Philosophical Transactions of the Royal Society A*, *378*, 20190358. https://doi.org/10.1098/rsta.2019.0358

van der Zee, C., & van Raaphorst, W. (2004). Manganese oxide reactivity in North Sea sediments. *Journal of Sea Research*, *52*(2), 73–85. https://doi.org/10.1016/j.seares.2003.10.005

von Appen, W.-J., Schauer, U., Hattermann, T., & Beszczynska-Möller, A. (2016). Seasonal cycle of mesoscale instability of the West Spitsbergen Current. *Journal of Physical Oceanography*, *46*(4), 1231–1254. https://doi.org/10.1175/JPO-D-15-0184.1

Vancoppenolle, M., Bopp, L., Madec, G., Dunne, J., Ilyina, T., Holloran, P. R., & Steiner, N. (2013). Future Arctic Ocean primary productivity from CMIP5 simulations: Uncertain outcome, but consistent mechanisms. *Biogeochemical Cycles*, *27*(3), 605–619. https://doi.org/10.1002/gbc.20055

Wang, Q., Wekerle, C., Wang, X., Danilov, S., Koldunov, N., Sein, D., et al. (2020). Intensification of the Atlantic Water Supply to the Arctic Ocean Through Fram Strait Induced by Arctic Sea Ice Decline. *Geophysical Research Letters*, *47*, e2019GL086682. https://doi.org/10.1029/2019GL086682

Wehrmann, L. M., Formolo, M. J., Owens, J. D., Raiswell, R., Ferdelman, T. G., Riedinger, N., & Lyons, T. W. (2014). Iron and manganese speciation and cycling in glacially influenced high-latitude fjord sediments (West Spitsbergen, Svalbard): Evidence for a benthic recycling-transport mechanism. *Geochimica et Cosmochimica Acta*, *141*, 628–655. https://doi.org/10.1016/j.gca.2014.06.007

Wiers, S., Snowball, I., O'Regan, M., & Almqvist, B. (2019). Late Pleistocene Chronology of Sediments From the Yermak Plateau and Uncertainty in Dating Based on Geomagnetic Excursions. *Geochemistry, Geophysics, Geosystems*, *20*, 3289–3310. https://doi.org/10.1029/2018GC007920